

# A Simple and Novel Route for Synthesis of Vanadium Carbide Nanoparticles

Haoyang Wu<sup>1\*</sup>, Zhiqin Cao<sup>2</sup>, Chengyang Zuo<sup>2</sup> and Xuefeng Zhang<sup>2</sup>

<sup>1</sup>Institute for Advanced Materials and Technology, University of Science and Technology, China

<sup>2</sup>School of Materials Science and Engineering, Pan Zhihua University, China

## Research Article

Received: 17/12/2018

Accepted: 01/01/2019

Published: 07/01/2019

### \*For Correspondence

Institute for Advanced Materials and Technology,  
University of Science and Technology Beijing,  
China.

**Tel:** +86 (812) 337 1000

**E-mail:** wuhaoyang@ustb.edu.cn

**Keywords:** VC nanoparticles, Carbothermal reduction, Combustion synthesis, Precursor

### ABSTRACT

Vanadium carbide (VC) nanoparticles were prepared via a simple and novel route by solution combustion synthesis and carbothermal reduction method for the first time. The prepared precursor consisted of flake particles with a uniform dispersion of vanadium, oxygen and carbon. The precursor powders was subsequently calcined under nitrogen at 700-1200 °C for 3 h. During the carbothermal reduction process, the phase changed from  $V_2O_5$ ,  $VO_2$ ,  $V_2O_3$  to VC. At the temperature of 1200 °C, the pure-phase of VC was successfully prepared. The sizes of prepared VC nanoparticles are less than 30 nm. This new approach to prepare nanocrystalline VC is suitable for large scale production of VC nanoparticles.

## INTRODUCTION

Vanadium carbide (VC) is particularly important for industrial applications due to its excellent high temperature strength, high thermal and chemical stability even at high temperatures [1-5]. It has been widely used for cutting materials, abrasive and anti-wear materials. Meanwhile, VC is an extremely hard refractory ceramic material and can also be used as an additive to tungsten-base and titanium-base to fine the grain to improve the property of a cermet [6,7]. Moreover, VC exhibits catalytic behaviors, which are almost comparable to platinum metal owing to their similar electronic and magnetic properties [8-10]. Some researches indicated that vanadium carbides are much more efficient catalysts than traditional catalytic materials (Ni, Pt, Rh, etc.) for N-H bond activation due to the broadening of the d-band that would give vanadium carbides an opportunity to be better electron acceptors than the platinum group metals [11]. Due to its promising properties and extensive applications, it is worth to investigate various ways of synthesizing nanocrystalline VC with convenient manipulations. Various methods have been explored for the synthesis of VC such as carbothermal reaction, direct element reaction, mechanical alloying ion exchange route and thermal decomposition of the precursor etc. [12-16]. Among these methods, the most popular method for synthesizing the VC is the carbothermal reduction and this method is also regarded as an economical method for commercial production [17,18].

In this paper, it developed a simple and convenient route by combining solution combustion synthesis (SCS) and carbothermal reduction method to prepare VC nanoparticles. Solution combustion synthesis (SCS) is a well-known method for the preparation of nanocrystalline oxides [19]. This method has a lot of advantages. The reaction of SCS is an exothermic reaction. It saves energy because the heat needed to drive the chemical reaction is provided by itself and not by an external source; the combustion reaction is instantaneous; and the production exhibits high specific surface area, well-defined chemical compositions, and homogeneous distribution of the elements [20-22]. During the recent years, some researchers began to employ the SCS method to prepare non-oxide ceramic powder. We have successfully synthesized nitrides by the combination of combustion synthesis and carbothermal reduction [23-26]. In the present work, the synthesis of VC nanoparticles by SCS and carbothermal reduction method has been investigated for the first time. Firstly, a homogeneous mixture of vanadium oxide and carbon precursor was prepared by SCS. Subsequently, the prepared precursor was carbothermally reduced to VC particles.

## EXPERIMENTAL SECTION

### Synthesis

Precursor was prepared by SCS using ammonium vanadate ( $\text{NH}_4\text{VO}_3$ ), ammonium nitrate ( $\text{NH}_4\text{NO}_3$ ), glycine ( $\text{NH}_2\text{CH}_2\text{COOH}$ ) and glucose ( $\text{C}_6\text{H}_{12}\text{O}_6$ ) as raw materials. Analytical reagent grade chemicals were purchased commercially. As a typical sample preparation procedure, 5.8 g  $\text{NH}_4\text{VO}_3$ , 24 g  $\text{NH}_4\text{NO}_3$ , 12 g  $\text{NH}_2\text{CH}_2\text{COOH}$  and 30 g  $\text{C}_6\text{H}_{12}\text{O}_6$  were dissolved in deionized water under stirring to obtain a redox mixture. The mixture was filled into a glass, and was heated in air on a temperature-controlled electrical furnace. The experimental phenomenon were similar with the previous reports [27,28]. The whole process took only several minutes, resulting in a fragile and foamy products (precursor). The carbonization of precursor was performed in a tube furnace. A strict temperature program was followed in all runs, with heating at a constant rate of  $10 \text{ K min}^{-1}$  up to the plateau temperature. The precursor was calcined in a flowing  $\text{N}_2$  at various temperatures for 3 h.

### Characterizations

The products were analyzed by X-ray diffractometer using  $\text{Cu-K}\alpha$  ( $\lambda=0.1542 \text{ nm}$ ) radiation [X-ray diffraction (XRD); Rigaku, D/max-RB12] and Thermo Gravimetric Analysis (TGA)/differential scanning calorimetry (DSC) (MettlerToledo, Switzerland). The morphology and particle size of the prepared products were studied by scanning electron microscopy (SEM, JSM-5600) and transmission electron microscopy (TEM, Tecnai G2 F30 S-TWIN). The specific surface area (SSA) of the precursor was determined by the Brunauer-Emmett-Teller (BET) method using an automated surface area and pore size analyzer (QUADRASORB SI-MP, Quantachrome Instruments, Boynton Beach, FL). The X-ray photoelectron spectroscopy (XPS) analysis was carried out using AXIS Ultra DLD spectrometer equipped with an  $\text{Al K}\alpha$  X-ray source and electrostatic hemispherical electron analyzer.

## RESULTS AND DISCUSSION

### Preparation of the Precursor

**Figure 1** shows the X-ray diffraction (XRD) pattern of the precursor prepared by SCS. It indicates that the precursor is composed of  $\text{V}_2\text{O}_5$  and  $\text{VO}_2$ . It is well known that SCS is in essence a redox exothermic reaction between oxidizer and reducer. During heating, the redox reaction between ammonium vanadate, ammonium nitrate and glycine occurs. Eq.1 describes this reaction in a simple manner. Because of the energy released from the exothermic reaction, the glucose decomposes (Eq.2) and carbon generated from the glucose reacts with the  $\text{V}_2\text{O}_5$  (Eq.3). The  $\text{V}_2\text{O}_5$  has been reduced to  $\text{VO}_2$ . Meanwhile, a part of carbon has been oxidized, as shown in Eq.4. In this way, a precursor that contains the mixture of  $\text{V}_2\text{O}_5$ ,  $\text{VO}_2$  and carbon can be obtained. Moreover, a large volume of gases liberated during the reactions would effectively prevent the agglomeration of particles, rendering the formation of porous, fragile, foamy, and black precursor.

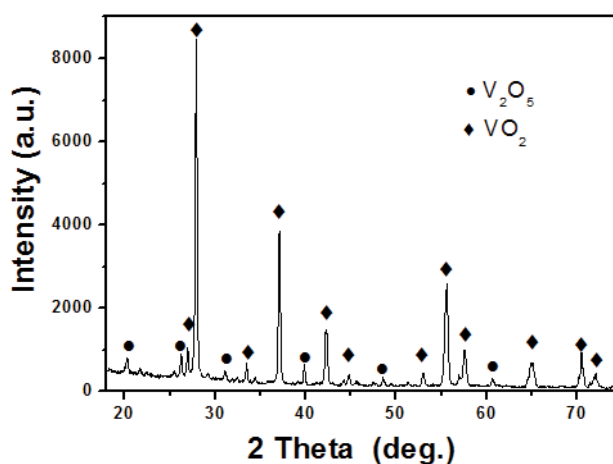


**Figure 1.** XRD pattern of the precursor.

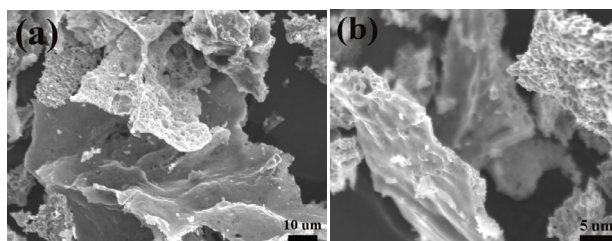


**Figure 2.** SEM photograph of the precursor.

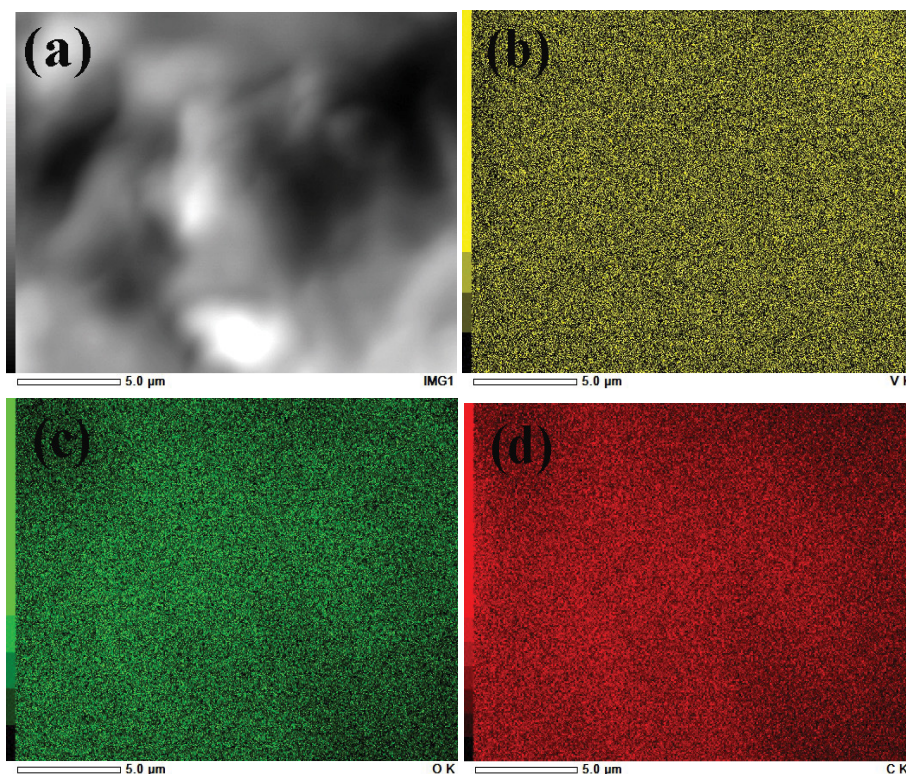
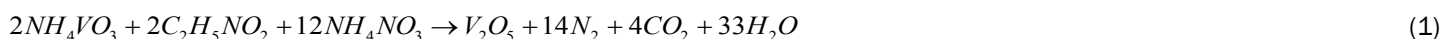


**Figure 3.** EDS element mapping data of (a) SEM image of the precursor, (b) V, (c) O and (d) C elements throughout the precursor.

**Figure 2** presents the SEM images of the precursor. The precursor has a porous structure (**Figure 2a**) and consists of flaky particles with an average thickness of about 2 μm (**Figure 2b**). The specific surface area of the precursor is 6 m<sup>2</sup>/g. **Figure 3** shows the map distribution of V, O and C elements. It is evident that the precursor has homogeneous distribution of V, O and C. Intimate contact between the vanadium and the carbon can decrease the diffusion distance between the reactants and improve the reactivity.



**Synthesis of Vanadium Carbide Nanoparticles**

**Figure 4** shows the TG and DSC curves of the precursor in N<sub>2</sub> atmosphere. It is clear that sample undergoes a mass loss of ~7% before 300 °C due to the adsorbed water evaporation. Increasing calcined temperature to 1200 °C, the sample gradually loses a large of mass of 68% and maintain stable.

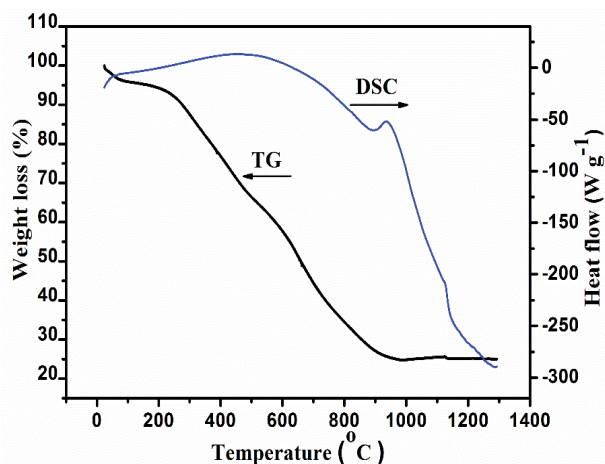


**Figure 4.** TG and DSC curves of the precursor in N<sub>2</sub> atmosphere.

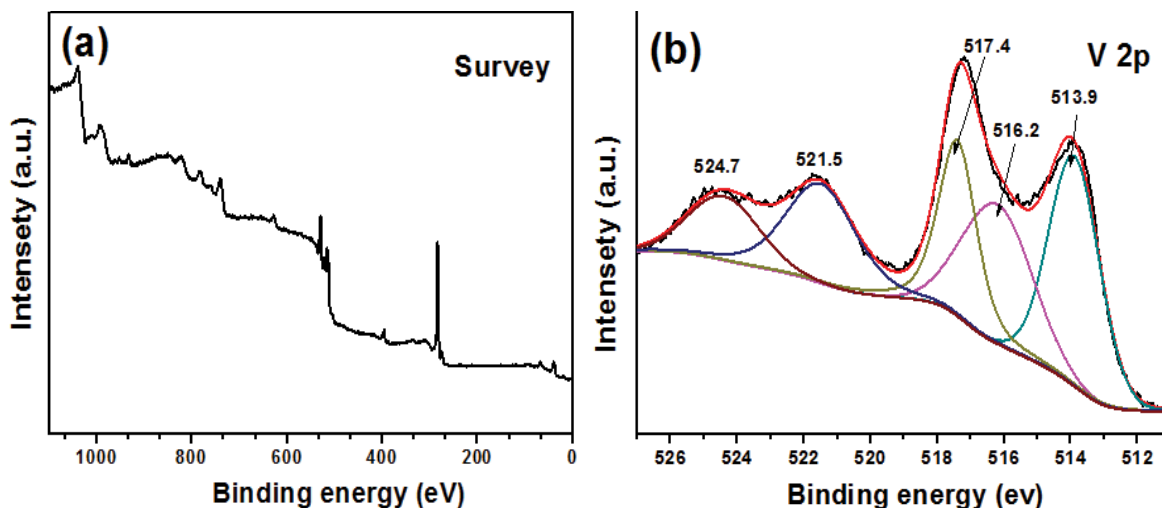


Figure 5. XRD patterns of the carbonization products calcined at various temperature.

Figure 5 demonstrates the X-ray diffraction analysis of the products calcined at 700-1200 °C. The sample, calcined at 700 °C, is comprised of single phase  $V_2O_3$ . It indicates that the precursor has been reduced to  $V_2O_3$ . The reaction is shown in Eq.5. At the temperature of 900 and 1100 °C, the samples are mainly comprised of VC and the weak diffraction peaks of  $V_2O_3$  also appear, indicating the transformation of  $V_2O_3$  to VC (Eq.6). The vanadium oxide phases cannot be detected in the XRD pattern of the sample calcined at 1200 °C (Figure 4). All the sharp reflection peaks can be indexed to the VC compound (PDF NO. 65-8074) and the pure-phase of VC is prepared at 1200 °C.

XPS was used to study the components and surface properties of the products. Figure 6 shows several regions of the XPS spectra of the products prepared at 1200 °C. Wide survey scans (Figure 6a) identified the presence of vanadium (V 2p), carbon (C 1s), and oxygen (O 1s). Figure 6b depicts the XPS spectra of V 2p. Peaks at 513.9 and 521.5 eV should result from V 2p<sup>3/2</sup> and V 2p<sup>1/2</sup> spin-orbit component of VC respectively [29]. The peaks at 516.2, 517.4 and 523.7 eV are assigned to the V 2p species of  $V_2O_3$ ,  $VO_2$  and  $V_2O_5$  [30]. In Figure 6c, the peak of C 1s spectrum at 284.6 eV is attributed to the free carbon on the surface of the products and the peak at 282.5 eV is attributed to the photoelectrons ejected from the carbon in vanadium lattice [16,30]. Two peaks at 286.3 and 288.6 eV are assigned to the oxygen bound species C-O and C=O respectively [31]. The high-resolution O 1s spectrum is shown in Figure 6d and it indicates that the oxygen species not only include simple lattice oxygen (529.5 eV) but also at least include hydroxyl oxygen (532.0 eV) [16,29]. The XPS results confirm the formation of VC and there are oxygen on the surface of VC due to exposure to the air. The similar phenomenon has also been mentioned by other researches [16,29].

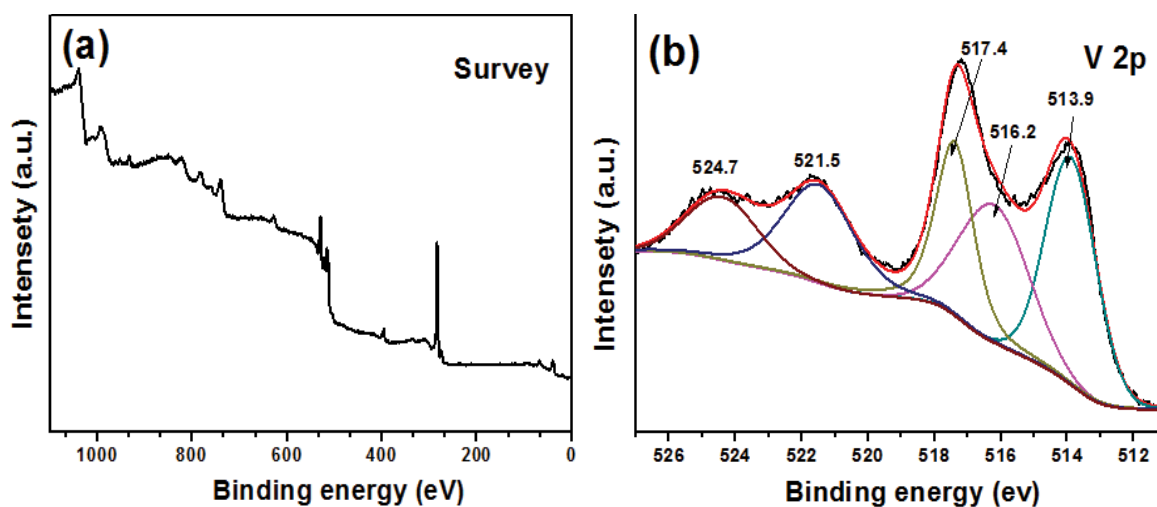
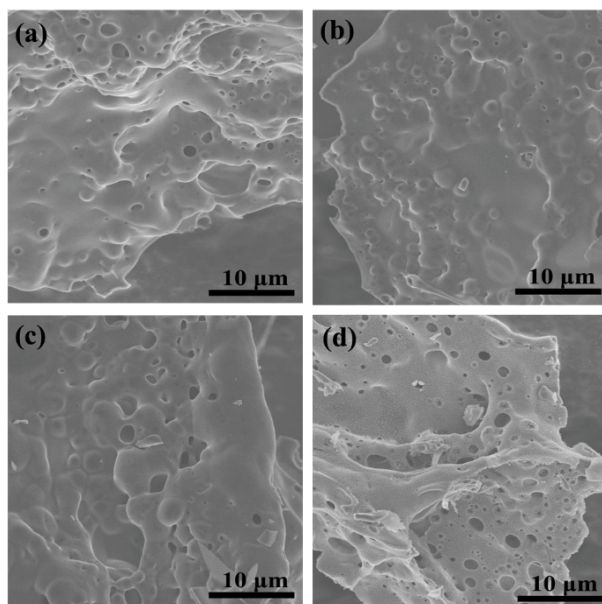
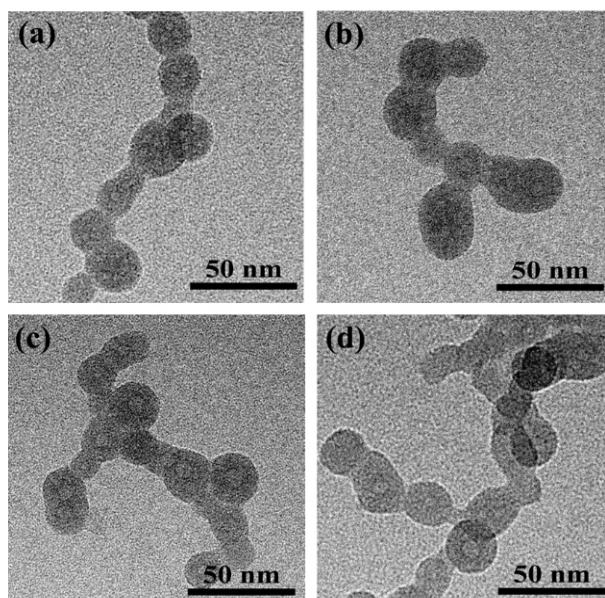


Figure 6. Wide (a) and narrow scan (b, c and d) XPS patterns for product prepared at 1200 °C.





**Figure 7.** SEM images of the carbonization products calcined at various temperature: (a)700 °C, (b) 900 °C, (c)1100 °C, (d)1200 °C.



**Figure 8.** TEM images of the carbonization products calcined at various temperature: (a)700 °C, (b) 900 °C, (c)1100 °C, (d)1200 °C.

The morphologies of the products calcined at different temperature are investigated by SEM and TEM. As shown in **Figure 7**, all the calcined products exhibit the sheet structure. From the TEM images (**Figure 8**), it can be also observed that the carbonization product calcined at 700 °C is comprised of nanoparticles of 20 nm. With increasing the calcined temperature up to 1200 °C, the particle sizes increase to 25~30 nm. The relatively low growth rate of VC particles can be attribute to the homogeneous distribution of carbon, which can inhibit the growth of VC nanoparticles during the calcined process.

**Figure 9** display the reaction mechanism of the carbonization process. was investigated by analyzing the phase transformation and microstructure evolution. (a) After combustion synthesis, vanadium oxides ( $VO_2$  and  $V_2O_5$ ) and carbon are homogeneous distribution and closely contacted with each other. (b) Due to the high contact area of vanadium oxides and carbon, carbon atoms did not need a long distance diffusion and  $V_2O_5$  and  $VO_2$  can be reduced to  $V_2O_3$  at a relative low temperature, which had been verified by the XRD results. During the reduction process, CO was formed and escaped from the reaction interface (eq. (5) and (6)). (c) With the increase of calcined temperature, carbon atoms entered into the lattice and occupied most of the lattice positions of oxygen atoms, resulting in forming VC. Therefore, part of  $V_2O_3$  in the surface of sample was carbonized to VC. (d) When the temperature increase up to 1200 °C, carbon atoms continued to enter into the lattice and  $V_2O_3$  has been absolutely carbonized to VC.



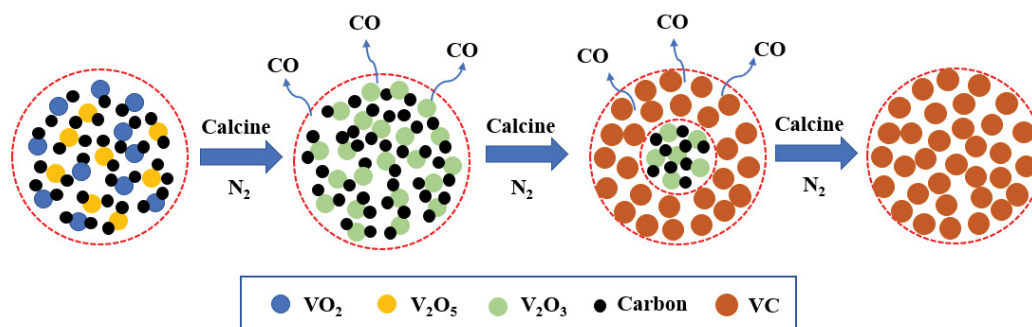


Figure 9. Reaction mechanism of the carbonization process.

## CONCLUSIONS

Vanadium carbide (VC) nanoparticles were prepared via a simple and novel route by carbothermal reduction of a combustion synthesized precursor. A homogeneous precursor had been prepared by solution combustion synthesis in a few minutes using ammonium vanadate, ammonium nitrate, glycine and glucose as raw materials. The precursor was subsequently calcined at 1200 °C under nitrogen and the pure-phase of VC was successfully prepared. The sizes of prepared VC nanoparticles were less than 30 nm. It provides a new approach to prepare nanocrystalline VC and is suitable for large scale production of VC nanoparticles.

## ACKNOWLEDGEMENTS

This work was supported by the National Natural Science Foundation Program of China (50802006) and (51172017), the National 863 Program (2013AA031101) and Science Foundation Program of Panzhihua (2014CY-G-26-2).

## REFERENCES

- Chen Y, et al. A simple and novel route to synthesize nano-vanadium carbide using magnesium powders, vanadium pentoxide and different carbon source. *Int J Refract Met Hard Mater.* 2011;29:528-531.
- Tang RZ, Research and the Latest Development of Gallium Recovery Process and Technology. *Rare Metals and Cemented Carbides.*2000;141:11-13.
- Lipatnikov VN, et al. Effects of vacancy ordering on structure and properties of vanadium carbide. *J Alloys Compd.* 261;1997:192-197.
- Kapoor R and Oyama ST. Synthesis Of Vanadium Carbide By Temperature-Programmed Reaction. *J Solid State Chem.* 1995;120:320-326.
- Sadangi RK, et al. Synthesis and analysis of high surface area Vanadium Carbide nanoparticles. *Adv in Powder Metal Part Mater.* 1998;9-15.
- Feng P, et al. Effect of VC addition on sinterability and microstructure of ultrafine Ti (C, N)-based cermets in spark plasma sintering. *J Alloys Compd.* 2008;460:453-459.
- Morton CW, et al. High Resolution Electron Microscopy Study in ZrC-Doped WC-12 mass%Co Alloys. *Int J Refract Met Hard Mater* 2005;23:287-293.
- Choi JG, Ammonia Decomposition over Vanadium Carbide Catalysts. *J Catal.* 1999; 82:104-116.
- Frantz P, et al. Coordination chemistry of transition metal carbide surfaces: detailed spectroscopic and theoretical investigations of CO adsorption on TiC and VC (100) surfaces. *J Phys Chem B.* 2002;6456-6464.
- P Rodríguez, et al. *Catalyst Communication.* 2004;5:79-82.
- Blomberg MRA, et al. PdEo, Pd CO. All-electron CPF level. Relativistic contributions to CO bin-ding 11 and 14 kcal/mol, resper~ive~y, originate from smaller 4d-4d 5s splitting. Pd and PdH tests. *Am Chem Soc* 1992;114:6095-6102.
- Zhao Z, et al. Numerical simulation and experimental analysis of gas/solid flow systems: 1999 Fluor-Daniel Plenary lecture. *Powder Techno.* 2008;181:31-35.
- Sun Y, et al. A facile route to carbon-coated vanadium carbide nanocapsules as microwave absorbers. *RSC Adv.* 2013;3:18082-18086.
- Zhang B and ZQ Li, Synthesis of vanadium carbide by mechanical alloying. *J Alloys Compd.* 2005;392:183-186.
- Yan Z, et al. An ion exchange route to produce carbon supported nanoscale vanadium carbide for electrocatalysis. *J Mater Chem.* 2011;21:19166-19170.

16. Zhao Z, et al. A novel method to synthesize vanadium carbide (V<sub>8</sub>C<sub>7</sub>) nanopowders by thermal processing NH<sub>4</sub>VO<sub>3</sub>, C<sub>6</sub>H<sub>12</sub>O<sub>6</sub> and urea. *J Alloys Compd.* 2009;468:58-63.
17. Berger LM, et al. Investigation of the effect of a nitrogen-containing atmosphere on the carbothermal reduction of titanium dioxide. 1999;17:235-243.
18. White GV, et al. Carbothermal synthesis of titanium nitride. *J Mater Sci.* 1992;27:4287-4294.
19. González Cortés SL, Imbert FE, Fundamentals, properties and applications of solid catalysts prepared by solution combustion synthesis (SCS). *Appl Catal .* 2013;452:117-131.
20. Fumo DA, et al. Combustion Synthesis of Iron-Substituted Strontium Titanate Pervoskites. *Mater Res Bull* 10. 1997; 1459-1470.
21. Purohit RD, et al. Ultrafine ceria powders via glycine-nitrate combustion. *Materials Research Bulletin.* 2001;15:2711-2721.
22. Chakraborty A, et al. Quantitative versus subjective evaluation of mammography accreditation phantom images. *J Material Reseach.* 1995;4918-4922.
23. Chu A, et al. Citric Acid-Assisted Combustion-Carbothermal Synthesis of Well-Distributed Highly Sinterable AlN Nanopowders. *J Am Ceram Soc* 2012;95:2510-2515.
24. Qin M, et al. AlN powder synthesis by sodium fluoride-assisted carbothermal combustion. *Mater Res Bull.* 2008;43:2954-2960.
25. Chu A, et al. N-acenodithiophene and Acenaphthoquinoline for Efficient Polymer Solar Cells Application. *Mater Charact.* 2013;81:76-84.
26. Chu A. Effect of aluminum source on the synthesis of AlN powders from combustion synthesis precursors. *Mater Res Bull.* 2012;47:2475-2479.
27. Cao Z, et al. Facile route for synthesis of mesoporous Cr<sub>2</sub>O<sub>3</sub> sheet as anode materials for Li-ion batteries. *Electrochim Acta.* 2014;139:76-81.
28. Cao Z, et al. *Nanoparticle Research.* 2015;17,
29. Liu F. A high current anodization to fabricate a nano-porous structure on the surface of Ti-based implants. *J Mater Sci.* 2011;46:3693-3697.
30. Choi JG. The surface properties of vanadium compounds X-ray photo electron spectroscopy. *Appl Surf Sci.* 1999;148:64-72.
31. Zhao L. One-step solvothermal synthesis of a carbon@TiO<sub>2</sub> dyade structure effectively promoting visible-light photocatalysis. *Adv Mater.* 2010;22:3317-3321.